UNIVERSITY OF TWENTE.

Mulloon Institute
For environment, farming and society.

THE EFFECT OF LEAKY WEIRS ON GROUNDWATER TABLES IN THE MULLOON CATCHMENT

by

Jochem Meinen
s2394839

A Bachelor Thesis, Submitted in Partial Fulfilment of the Requirements for the Degree of

Civil Engineering

In the Faculty of Engineering Technology

Supervisors

Dr. ir. D.C.M Augustijn *(replaced Dr. ir. M. Pezij on 10-11-2022)*

L. Peel

Dr. ir. M. Pezij

Second assessor

Dr. M. van Buiten

UNIVERSITY OF TWENTE

November 11th, 2022

SUMMARY

This thesis is about the leaky weir structures installed in Mulloon creek and their effect on the groundwater in Mulloon catchment. 38 piezometers, 2 rain gauges, and a stream gauge installed in the catchment have been gathering data over varying periods between December 2015 and September 2022. This report describes the process of a Pearson correlation analysis, a time series cross-correlation analysis, and a quantitative analysis of the change in water height in the piezometers relative to either rainfall in millimeters over a day or to the number of days without rainfall.

The correlation analysis found 207 pairs of piezometers correlated .85 or above. This list was shortened to a group of 44 pairs of piezometers based on whether the water height in a piezometer in a pair was correlated .85 or above with the water height in the stream. This list of 44 piezometer pairs was then used in the cross-correlation analysis. The result of this analysis were lag times between piezometers. The list of 44 piezometers was then also used in the quantitative analysis.

The correlation analysis showed that there probably is some form of flow between groundwater aquifers in the catchment. The cross-correlation analysis showed that there probably is no flow between transect 2 and transect 4, but there might be a flow between transect 3 and transect 4. Tracer tests could give conclusive evidence on this subject.
When looking at all available data, the quantitative analysis showed that the recharge rate of most piezometers and the discharge rate of some piezometers increased after the leaky weirs were installed. When only looking at the data from the dry period, the increase in the recharge rate was not present anymore, but the increase in the discharge rate was still observed. This suggests that the weather that the catchment experiences has a large influence on these rates. In the future, the analysis should be repeated for post-leaky weir periods that are similar in weather to the pre-leaky weir periods.

The conclusion of this research is that there is likely flow between several groundwater aquifers in the catchment, but which aquifers those may be is yet undefined and the effect of the leaky weirs on these flows thus remains unknown. Also, the leaky weirs may have an effect on the recharge and discharge rates of the piezometers, however for conclusive evidence the analysis has to be repeated on a dataset with limited variability in rainfall.

CONTENTS

1. Context: European settlers and agriculture

For the past years, Australia has been dealing with decreasing water tables. European settlers have reduced the amount of vegetation significantly (Brierley et al. 1999) which in turn has increased erosion in stream beds (Dobes et al. 2013), see Figure 1. This can result in a decreasing water table due to a separation of the stream from the local groundwater (Dobes et al. 2013; Streeton et al. 2013). This separation has been shown to increase the consequences of dry periods and wildfires (Hazell, Osborne, and Lindenmayer 2003; Nolan et al. 2016). On top of this, rainfall in Australia falls in short bursts (Dunkerley 2018) and dry soil absorbs less rain (Burch, Moore, and Burns 1989). Periods of low precipitation increase the amount of dry soil, which leads to more runoff and erosion. Landscapes suffering from dry soil could benefit from higher groundwater tables (Dobes et al. 2013), because it would keep the soil moisture content higher, reducing the likelihood of the soil becoming too dry (Burch, Moore, and Burns 1989; Dobes et al. 2013). Initiatives aiming to increase the available groundwater volume in areas affected by these negative feedback loops should therefore be studied and implemented.

Figure 1 - soil erosion of pasture land in south Australia (Scott n.d.)

2. Research area

2.1 Geographic location of the study area

The study area is located in the Mulloon catchment, which is in the South-West of the state of New South Wales (NSW) in Australia. The Mulloon creek originates from this catchment, which is a tributary to the Shoalhaven river. The creek flows from south to north. Figure 2 shows an overview of the location of the Mulloon catchment relative to Canberra and Sydney (bottom right square). The research focuses on the Mid Mulloon and Lower Mulloon areas. These areas stretch from a point a few hundred meters of Kings Highway (B52) up to the point where the Mulloon Creek and Sandhills Creek join to form Reedy Creek. Figure 2 shows an overview of how Mid and Lower Mulloon are situated within NSW (top left square).

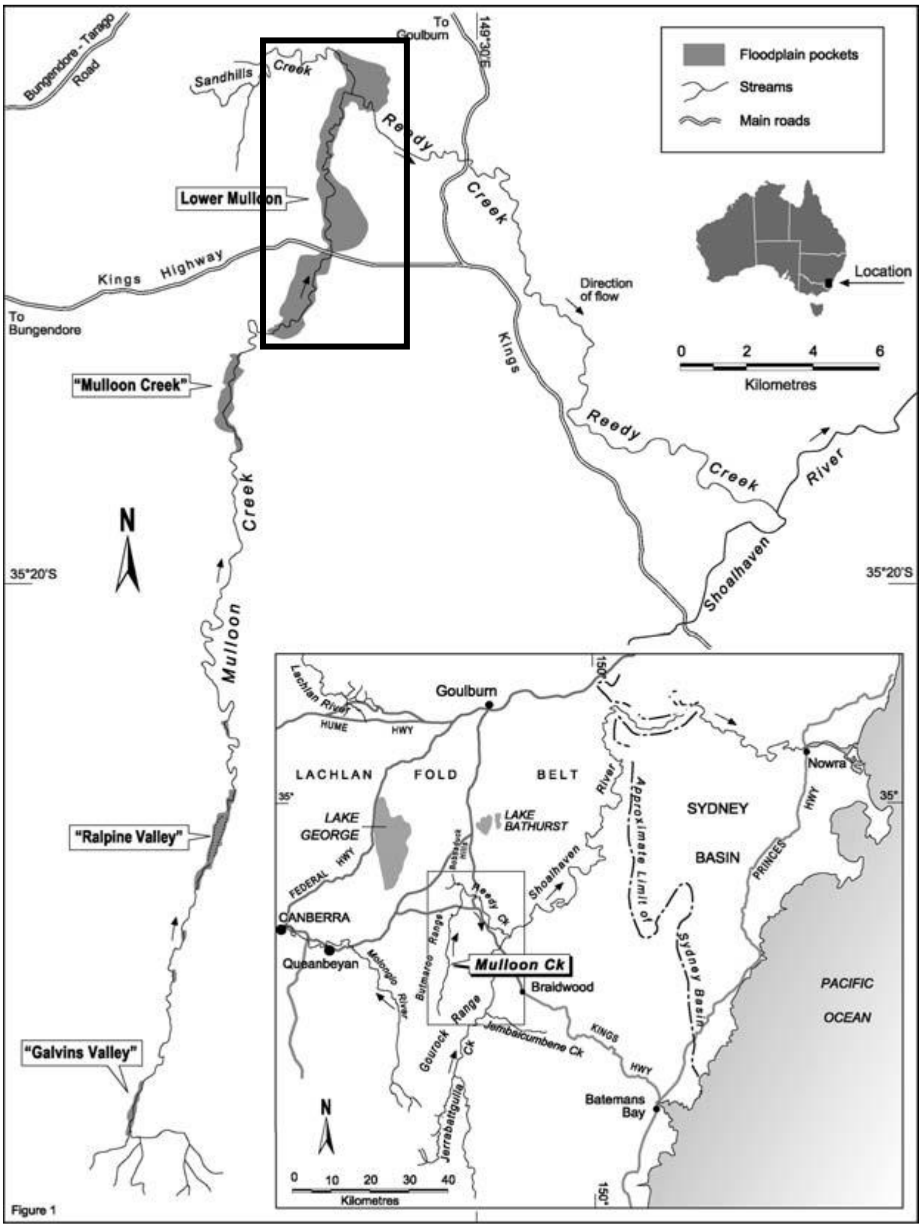

Figure 2 – the regional setting of the Mulloon Catchment (Johnston and Brierley 2006)

2.2 Instrument locations

38 piezometers, two rain gauges, and one stream gauge are situated in the study area, see Figure 3. They are again shown in Figure 4, which is a satellite image. The difference between Figure 3 and Figure 4 is that Figure 4 only shows the data sources used in this study, whereas Figure 3 shows all the instrumentation that is installed in the Mulloon catchment.

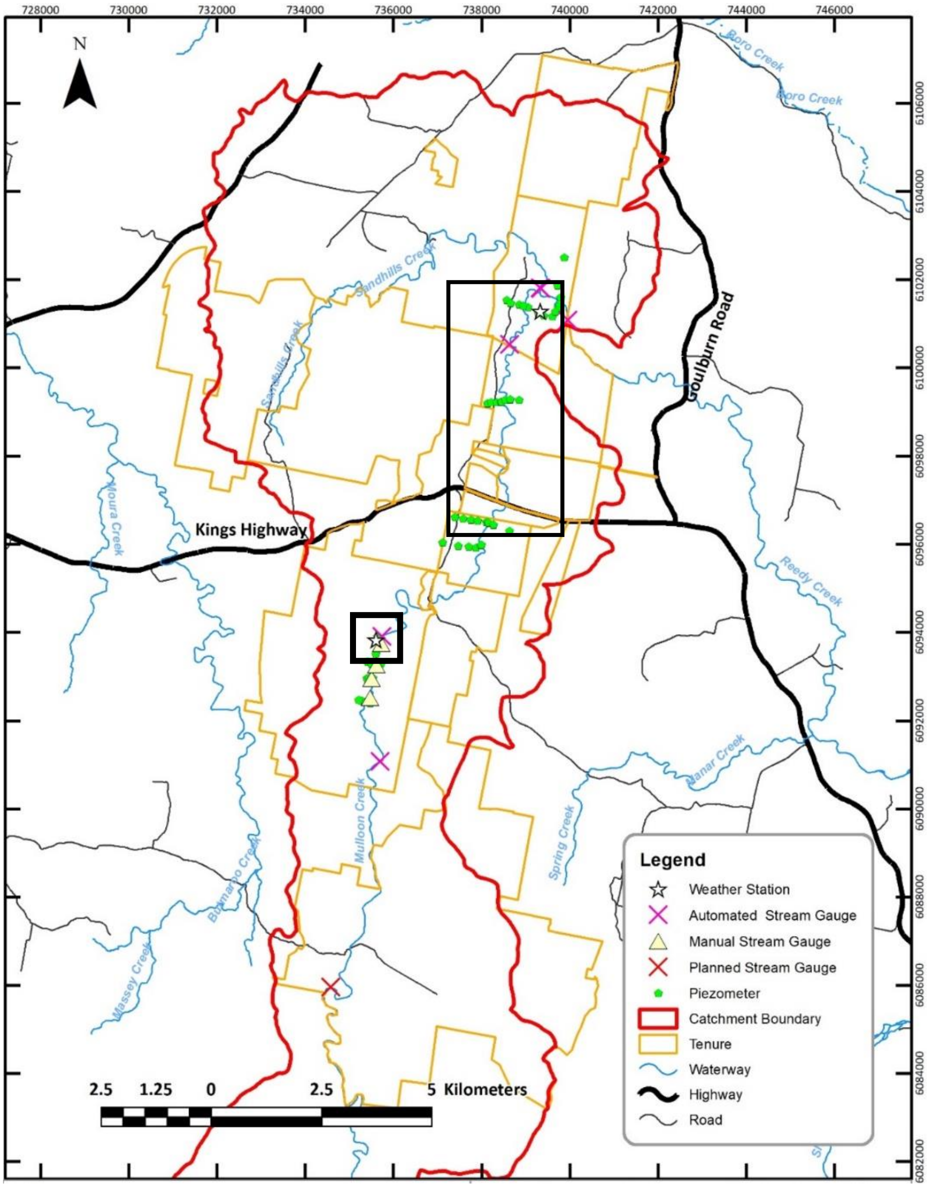

Figure 3 – The Mulloon catchment (L. Peel, personal communication, Sep 10, 2021)

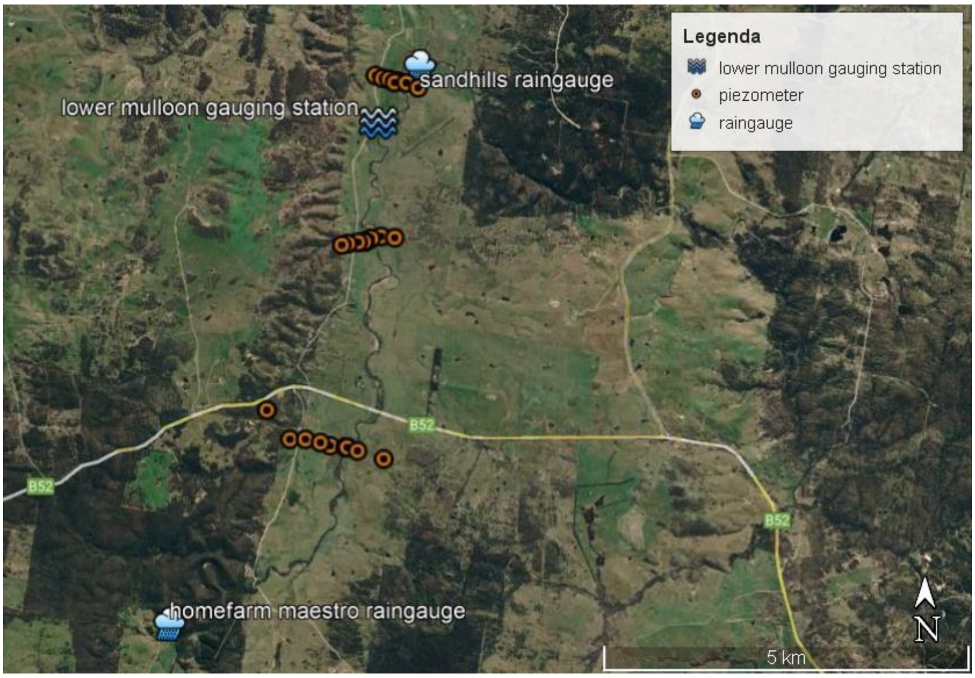

Figure 4 - 3 transects and 3 measuring stations (Google Earth, 2022)

The 43 piezometers are placed in three distinct lines that are perpendicular to the flow of the stream. These lines are referred to as transects and they are identified as T2, T3 and T4 from north to south. For reference, 5 transects exist in the Mulloon catchment, but T1 and T5 are not included in this research, because T1 was set up as an experiment and not meant for this type of research and the data from T5 has not yet been released. Table 1 lists all the piezometers that are used in this research.

Table 1 - piezometers used in this research

T2	T3	T4
MCLRP 26	MCLRP 38	MCLRP 49
MCLRP 27	MCLRP 39	MCLRP 50
MCLRP 28	MCLRP 40	MCLRP 51
MCLRP 29	MCLRP 41-1	MCLRP 52
MCLRP 30-1	MCLRP 42-1	MCLRP 53
MCLRP 30-2	MCLRP 43	MCLRP 54
MCLRP 31	MCLRP 44	MCLRP 55
MCLRP 32-1	MCLRP 45	MCLRP 56
MCLRP 32-2	MCLRP 46	MCLRP 57
MCLRP 33	MCLRP 47	MCLRP 58
MCLRP 34	MCLRP 48	MCLRP 59
MCLRP 35		MCLRP 60
MCLRP 36		MCLRP 77
MCLRP 37		

Figure 5 has all the piezometers together in 3d space. In the figure, the blue line gives a rough approximation of Mulloon Creek, the brown lines are a rough approximation of the ground surface. The transects from left to right are T4, T3, and T2. As can be seen, each transect is roughly parallel to the

Easting axis. In Figure 5 the rough shape of the terrain is also visible. The study area is a basin-shaped area of land with the stream at the bottom and T3 is at the thinnest part of the catchment.

The black lines in the figure are the piezometers and they show to what depth the piezometers are drilled. A mix of slotted and non-slotted piezometers is available. This means that the bottom of the black line is not necessarily from where the hydraulic head is measured.

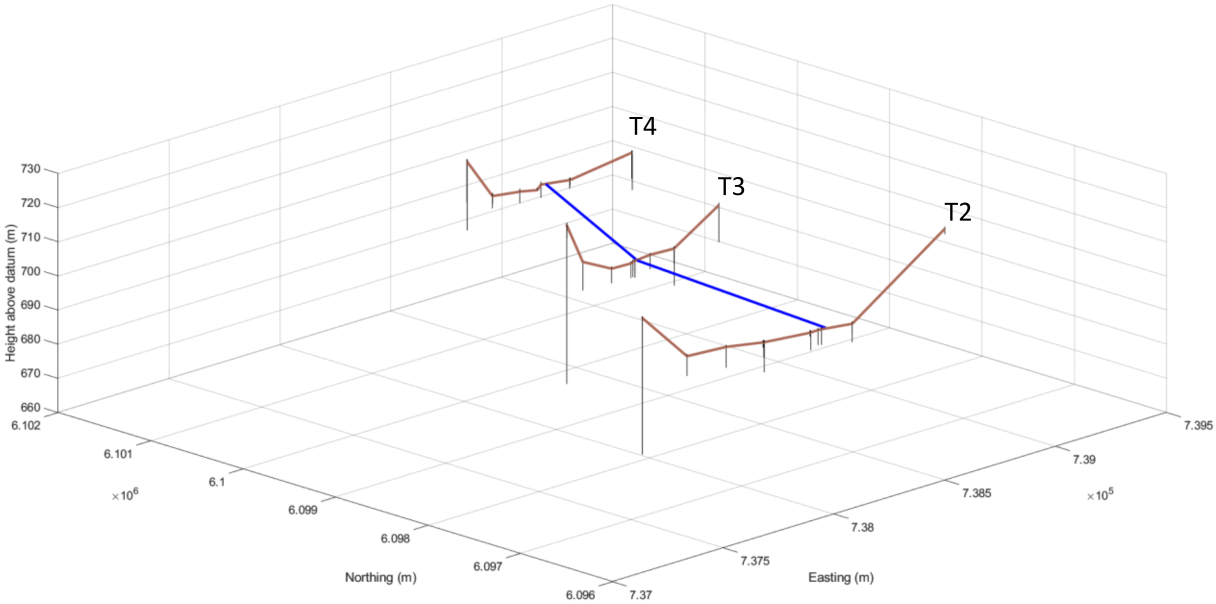

Figure 5 – 43 piezometers (black) and an approximation of the natural surface (brown) and Mulloon creek (blue) shown in 3d space

Figure 6 is a picture taken from inside T3. It has MCLRP 45 in the foreground with the recognizable blue monument of the piezometers, as mentioned in section 3.3. In the background, three more clusters of piezometers are visible, each is marked with an arrow. Figure 7 is a satellite image and it shows where the picture was taken. It also has the same three arrows pointing to the same three clusters of piezometers. The arrows are pointing to:

- Orange: 42-1, 42-2, 43 and 44
- Yellow: 41-1 and 41-2
- Blue: 40

Beyond the third arrow, a cluster with MCLRP 38 and 39 is present, although it is not visible in the picture. The picture gives an idea of the area in which the transects are placed. All piezometers that are visible except for 40 are in the floodplain. From MCLRP 40 and beyond the piezometers are drilled into the elevated ground. In the background of the picture is the Eastern ridge of the catchment. The Mulloon creek is between the white work vehicle and the orange arrow. Before the clearings that prepared the land for agriculture, part of this floodplain used to be a swamp with a discontinuous watercourse (Peel et al. 2022).

Figure 6 - Part of T3 with MCLRP 45 in the foreground (own photo)

Figure 7 - Schematic overview of picture of MCLRP 45 (Google Earth, 2022).

Throughout this report, all coordinates shown are cartesian. The system that is used is a grid reference system with the GDA2020 static datum, which was introduced in 2017 (ICSM 2022). The Z-coordinates are in meters above the Australian Height Datum (mAHD). All piezometer data shown in this research is in mAHD.

The whole of the study area lies between 734700 to 739800 meters Easting, 6092200 to 6102200 meters Northing, and 660 to 730 meters above datum.

2.3 Meteorological conditions

The whole of Australia, including the research area, has had a significant change in weather in the period 2017 through 2022. In 2018 and 2019 Australia experienced El Niño years and in 2020, 2021 and 2022 Australia experienced La Niña years. These two terms describe states of the El Niño Southern Oscillation (Enso) (L'Heureux 2014). During an El Niño, less atmospheric moisture is available for rainfall and therefore these years are often drier than regular years. During a La Niña, the weather conditions are reversed and a lot of atmospheric moisture is carried to Australia. Therefore, these years are often wetter than regular years. Henceforth the El Niño years are referred to as the dry period and the La Niña years are referred to as the wet period.

As can be seen in Table 2, the leaky weirs were constructed around the same time as Australia got out of the dry period and moved to the wet period. The leaky weirs that are referred to in Table 2 are the leaky weirs that are constructed within 1 kilometer upstream of where a transect crosses Mulloon creek.

Table 2 - leaky weir and instrument installation dates

Transect	Leaky weir construction finished	Instrument installation finished
2	1-12-2018	27-4-2017
3	1-12-2019	1-5-2017
4	1-9-2020/1-12-2020	3-11-2020

3. Problem statement

3.1 Problems in the Mulloon catchment and MRI

Like other parts of Australia, the Mulloon catchment has been dealing with the impacts of agriculture since the 21st century (Peel et al. 2022). There was a noticeable increase in runoff and the Mulloon creek that flows through the catchment was eroded to the point where it had turned from a discontinuous watercourse to a single, continuous stream. This increased the runoff of the catchment and caused a loss of nutrients in the soil and a loss of vegetation (diversity) (Peel et al. 2022). See Figure 8 for an example of streambed erosion in Mulloon creek.

Figure 8 – streambed erosion at transect 2 (own photo)

To combat these developments, the Mulloon Rehydration Initiative (MRI) was started in 2005. MRI is a long-term, catchment-scale stream and floodplain rehabilitation initiative (Peel et al. 2022). The focus of the initiative is to install in-stream structures and monitor their impact on hydrological, ecological, agricultural, and social values. These structures are called leaky weirs, more on them in section 3.2. To monitor the impact the leaky weirs have, long-term environmental research and monitoring have been taking place since the start of the project in 2005.

The problem that will be addressed in this research is the gap in knowledge about the leaky weirs with regards to their effect on the local groundwater. The data gathered through the Mulloon Rehydration Initiative is used in this research.

3.2 Leaky weirs

Leaky weirs are streambed erosion control structures (Peel et al. 2022), see Figure 9 for a picture of a leaky weir under construction and Figure 10 for a picture of a finished leaky weir. They are often made from logs, boulders, soil, and plants. The weirs were constructed in the Mulloon catchment to slow the drainage of rainfall from the catchment. The weirs lower the velocity of the water, increase water height and thus allow more water to be absorbed into the soil (Dobes et al. 2013; Peel et al. 2022). In practice, this has yielded promising results by reducing the water velocity, bank erosion rate, and salinity Peel et al. (2022).

Over the past 16 years, 60 leaky weirs have been constructed into a 50-kilometer stretch of Mulloon Creek. Each of them is between 0.4 and 0.6 meters. The distance between two leaky weirs is between 150 and 350 meters.

Figure 9 - leaky weir under construction at Westview farm (The Mulloon Institute, 2018)

Figure 10 - leaky weir at T2 (own photo)

3.3 Piezometers

Piezometers are boreholes filled with a solid casing and a screened casing. The screened casing is either screened to within 1 meter below ground level, or it is screened to an aquifer of interest. The casings contain a vented pressure transducer. They are vented to ensure that the recorded pressure in the borehole is relative to the atmospheric pressure. Above the surface level, the borehole is covered with a blue monument for protection against the weather and cattle.

Two types of piezometers exist that are classified by the screening depth that is used. Figure 11 shows the schematic for MCLRP 34, which was screened to within 1m of the surface level. Figure 12 shows the schematic for MCLRP 39, which was screened to a particular aquifer. These schematics also show how the piezometers are layered.

Lastly, the piezometers are sometimes clustered. Clustered means that there are several piezometers on a small surface area. This was done to have piezometers of different types or depths in the same location.

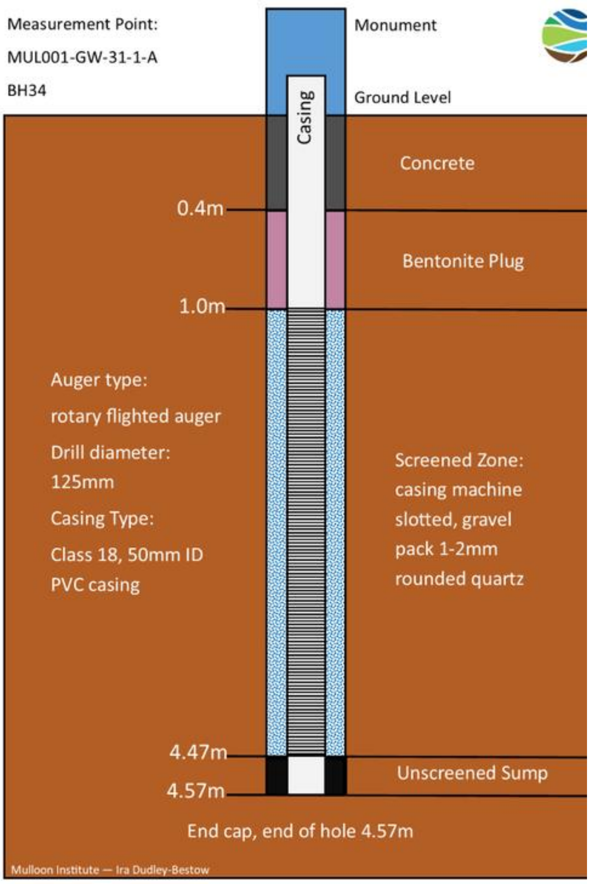

Figure 11 - MCLRP 34 schematic

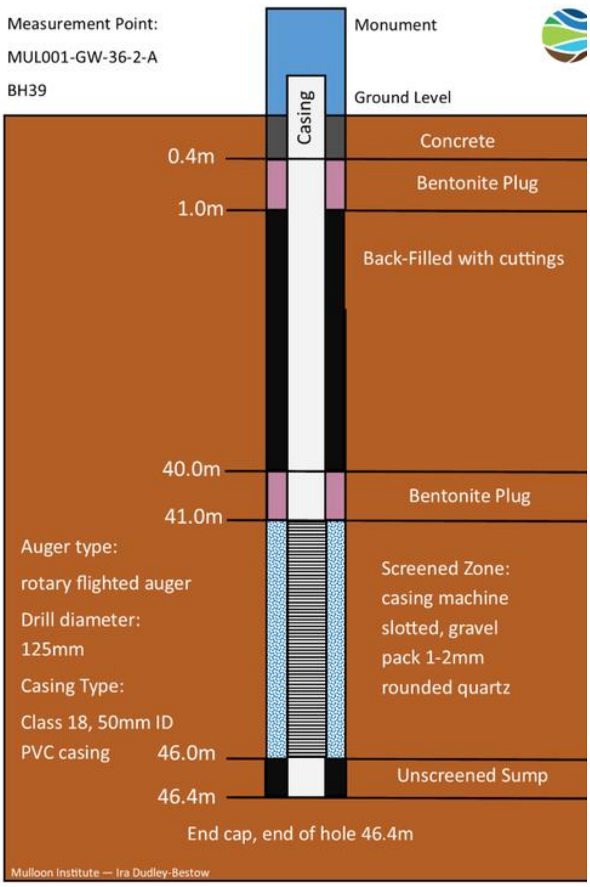

Figure 12 - MCLRP 39 schematic

4. Research questions

4.1 Main research question

One main research question follows from the problem statement:

What effect do leaky weirs in Mulloon Creek have on the interaction between the groundwater aquifers and the surface water?

4.2 Sub questions

To answer the main question the following questions are considered:

1. Is there flow between groundwater aquifers?
2. How much does the water height in the piezometers change after rain and after a dry period?
3. How much has the change in water height in the piezometers after rain and after a dry period been affected by the placement of leaky weirs?

5. Scope

The research will focus on transects 2 through 4 in the Mulloon catchment. The research consists of performing an analysis of the data gathered for each transect as well as the meteorological data collected from nearby weather stations and the water level data gathered by a stream gauge.

Furthermore, the research focuses on the influence that changes in the surface water table in Mulloon Creek have on the groundwater table of connected aquifers. Any other relationships or variables will not be taken into account.

Eventually, a model will be constructed of the area including the leaky weirs to predict changes to the ecosystem. A better understanding of the system and the effects leaky weirs have on the system should attribute to this goal. The model will be a geohydrological model, most likely constructed in APSIM. The construction of the model is not part of this research, but this research should contribute to the theoretical foundation of the model.

6. Methodology

The first step in looking at the data is to plot the monthly averages of each data source. This helps build an initial understanding of the data. Then, a tool is built to view the data as it was recorded, so per hour for the piezometers and stream gauge and per day for the rain gauges. This helps understand the response of the piezometers to specific events.

After visualizing the data, three analyses are performed, namely a Pearson correlation analysis, a cross-correlation analysis, and an analysis that looks at the rise and fall of the piezometers pre and post-leaky weir construction. The Pearson correlation analysis helps answer sub-question 1 because a correlation between two data sources is an indication of flow. The cross-correlation analysis also helps answer sub-question 1, because it can determine the direction of flow. The last analysis answers sub-question 2.

6.1 Monthly averages

The method used aggregates one data point per month for each time series in the research, a time series being the data recorded by a piezometer, rain gauge or stream gauge. This data point is the average of a month minus the average of the whole time series. It is the average deviation during a month from the total average. This way of displaying the data highlights trends over time and it helps with comparing the different piezometers with each other.

6.2 Pearson Correlation

For two time series (X, Y) like the time series for the piezometers, Pearson's correlation coefficient (ρ) is defined by Equation 1. In this equation, σ_X and σ_Y are the standard deviations of X and Y respectively. E is the expected value operator and μ_X and μ_Y are the expected values of X and Y respectively.

The result of the correlation analysis is a correlation matrix, where the variables are the water height in the stream in mAHD and the water height in the piezometers in mAHD. This makes the matrix 39x39: 38 piezometers and one stream gauge per axis.

$$\rho_{XY} = \frac{E[(X - \mu_X)(Y - \mu_Y)]}{\sigma_X \sigma_Y}$$

Equation 1 - Pearson's correlation coefficient

6.3 Cross-correlation

The goal of the cross-correlation analysis is to find a lag time between two piezometers and to determine what this lag time says about the interaction between the two piezometers.

For two time series (X_t, Y_t) like the time series of two piezometers, the cross-correlation function $\rho_{xy}(\tau)$ is defined by Equation 2. In this equation, τ is the delay in hours, and σ_X and σ_Y are the standard deviations of X_t and Y_t respectively. E is the expected value operator and μ_X and μ_Y are the expected values of X_t and Y_t respectively. The Cross-Correlation Function $\rho_{xy}(\tau)$ is here forth abbreviated with CCF.

$$\rho_{XY}(\tau) = \frac{E[(X_t - \mu_X)(Y_{t+\tau} - \mu_Y)]}{\sigma_X \sigma_Y}$$

Equation 2 – cross-correlation

For this analysis, the CCF is only calculated for subset of the piezometers. Which piezometers belong to this subset is listed in Table 5 in section 7.2. How this subset was chosen is also explained in section 7.2. The reason why this subset of piezometers was used instead of all of the piezometers is that it saves time. The cross-correlation involved doing a lot of steps by hand and doing this for all the piezometers would not have fit within the 10 week timeframe of this research.

The CCF is always calculated for two piezometers. In calculating the CCF, the length of the time series that the function is calculated for is limited to 10 days. This is because it often happens that the time series of a piezometer is not continuous or the time series of two piezometers do not share the same start and endpoints. Using an interval like 10 days increases the likelihood of taking a part of the time series of both piezometers that is continuous and complete. The reason a 10-day interval was chosen was that from visual observation of the data it was found that the peaks in the piezometers time series that emerged after rain usually fit within this period.

The 10-day intervals are determined based on big rainfall events. The 5th day of the interval always falls on a day that is logged as being in the top 5% of the biggest rain events in either of the two rain gauges. So if the amount of rain that fell on day x is in the top 5% out of all days recorded by one of the two rain gauges, then the interval for which the CCF is calculated is [x-4, x+5] where the interval is in days. In total, 18 days of heavy rain were used. This number is less than 5% of the number of days recorded by the rain gauges. This is because of two reasons. First, if two days in the top 5% fell within 10 days of each other, one of the two was excluded. Second, a lot of the days from the top 5% did not fall on days for which the piezometers recorded data.

Once the 10-day interval is determined, the maximum of the CCF is then calculated for τ in hours on the interval [-12, 12]. The lag time at this maximum is then recorded in a table along with the date x that determined the interval. The reason a 24h interval was chosen was that from visual observation it was found that the peaks in the time series of two piezometers usually happen within this period.

The goal of this analysis is to find a lag time per pair of piezometers that is accurate. To do this, the table discussed in the paragraph above can be used. This table would have the pair of piezometers as one variable, the date that the interval was based on as the other variable, and then the calculated lag time as a value. The next step is to take the median value of all the lag times per pair of piezometers. However, there are two problems. First, despite taking only a 10-day interval, there are still lots of instances where a CCF cannot be determined because the time series are not continuous or complete. This results in some pairs of piezometers that have almost no intervals for which lag times can be calculated. Second, for some pairs of piezometers, the lag times have very high standard deviations of several hours.

To account for the two problems, two criteria are included. The first criterion is to exclude all pairs of piezometers that have a sample size of less than 6 and the second criterion is to exclude all pairs where the standard deviation is less than 2.

6.4 Recharge and discharge rate

The leaky weirs that were installed had several expected effects, for example:

1. Rainwater is slowed down, allowing more water to infiltrate
2. Less water can flow from the groundwater reservoir into the stream

These effects should be visible in the recharge and discharge rates of the piezometers. The recharge rate is the rate at which the water height in the piezometers increases relative to a rainfall event. The discharge rate is the rate at which the water height in the piezometers decreases after the absence of rain. This rate is then calculated for each piezometer in the Group B as defined in section 7.2. This group is chosen because it saves time by excluding those piezometers that do not appear to be influenced much by the stream.

Calculating these two rates involves plotting points on a graph, drawing the trendline through the points and taking the slope of the trendline. For the recharge rate, the x-axis will have the amount of rain in millimeters and the y-axis will have the difference over 24 hours in the water height in a piezometer in meters. For the discharge rate, the x-axis will have the number of days with no rain and the y-axis will have the difference over that number of days in the water height in a piezometer in meters.

The goal of this analysis is to find if there are differences between the pre and the post-leaky weir periods. Therefore, the analysis is repeated per piezometer for different time period. The time periods that are chosen depend on which transect the piezometer is in. Table 2 in section **Error! Reference source not found.** defines per transect when the leaky weirs were installed and this date also serves as the point where the pre-period changes over into the post-period. Because the instrumentation for T4 was installed after the leaky weirs, there is no pre-period for the piezometers in T4 and thus they are excluded from the analysis.

To summarize, the analysis takes each piezometer in Group B, creates a discharge graph and a recharge graph for the pre-period and also for the post-period and calculates a trendline for each of these 4 graphs. The slope of these trendlines are recorded in a table.

For T2, there is a little over 1 year of data where the leaky weirs are installed but the catchment is still in the dry period. To see what the influence is of the weather on the recharge and discharge rates, this analysis is performed twice for the piezometers in T2. The second time the post-period does not span until the end of the time series, but until the wet season begins in February of 2020

7. Results

7.1 Monthly averages

As described in section 6.1, the graphs shown in this section depict the mean monthly deviation from the total mean of the time series. For the rainfall data this is done because it shows the difference between the dry and wet periods more clearly. For the piezometers this is done because it makes it easier to compare piezometers that are drilled in different heights in the landscape.

The first graph is the rainfall graph in Figure 13. The rain gauge higher up in the catchment is the orange 'homefarm spare' series and the rain gauge near T4 is the blue 'sandhills' series. The horizontal axis is divided into blocks of 3 months divided by light gray vertical lines. The month under the left line of a block is the first month for which the mean monthly deviation is calculated.

There are some gaps in both sets of data, but there is no month where there is no data from either of the rain gauges, so they complement each other. Also, visually it is already apparent that the two data sources are mostly in agreement with each other about the amount of rain that has fallen each month. This is also reflected in the correlation coefficient in 12.1.

The graph clearly shows that the months from December of 2015 up to February of 2020 were a lot drier than the months from February of 2020 onwards. This coincides with the ENSO phases as discussed in **Error! Reference source not found.**. These two periods are distinguished with colored blocks, where the dry period is colored orange and the wet period is colored blue. The wet period actually begins with a flood event. Between the 7th and the 11th of February 2020, the Sandhills rain gauge recorded 104.6 millimeters of rain and the Homefarm rain gauge recorded 114.8 millimeters of rain. For reference, this is roughly the same amount of rain as was recorded in the entire six months prior to this flood. Sandhills recorded 104 millimeters of rain between the 1st of August 2019 and the 31st of January 2020 and Homefarm recorded 115,8 millimeters of rain in the same period.

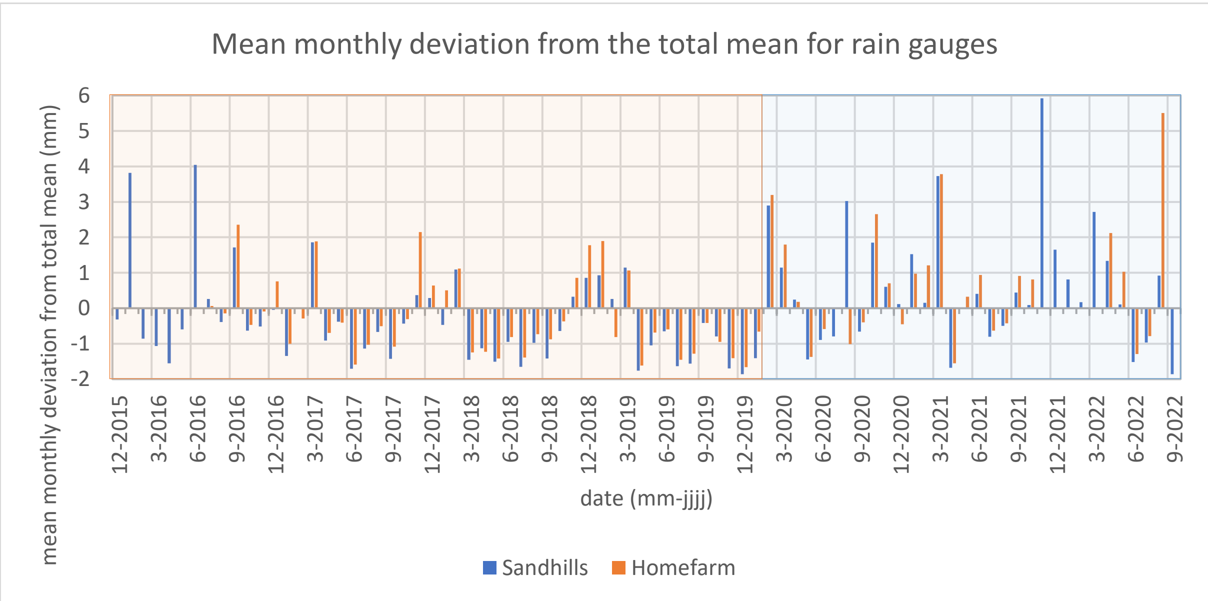

Figure 13 – mean monthly deviation from total mean of the rainfall

The second batch of graphs is of the three transects and they are shown in Figure 14, Figure 15, and Figure 16. For these graphs, extra black lines are added that show when leaky weir installation was completed. There are 4 black lines, one for T2 and T3 each and two for T4. These lines. These dates are the same as the ones shown in Table 2 in section **Error! Reference source not found.**. Also, in each graph, the stream gauge data is shown with a light blue dashed line. Lastly, the dry and wet periods are colored orange and blue respectively.

A sharp rise is visible for 5 piezometers in transect T2 and 6 piezometers in T3 in February of 2020, exactly when the flood happens and the wet season begins. For the two transects combined, this amounts to 11 out of the 13 piezometers that have data from December 2019 to April 2020. It is interesting to see that the spread of the piezometers during the dry period is small, but as soon as the wet period starts the spread gets bigger. This indicates that during a drought the water height in a piezometer rises and falls more in unison with its neighbors in the same transect than it does during a wet period. This is also reflected in the recharge-discharge analysis in section 7.4.

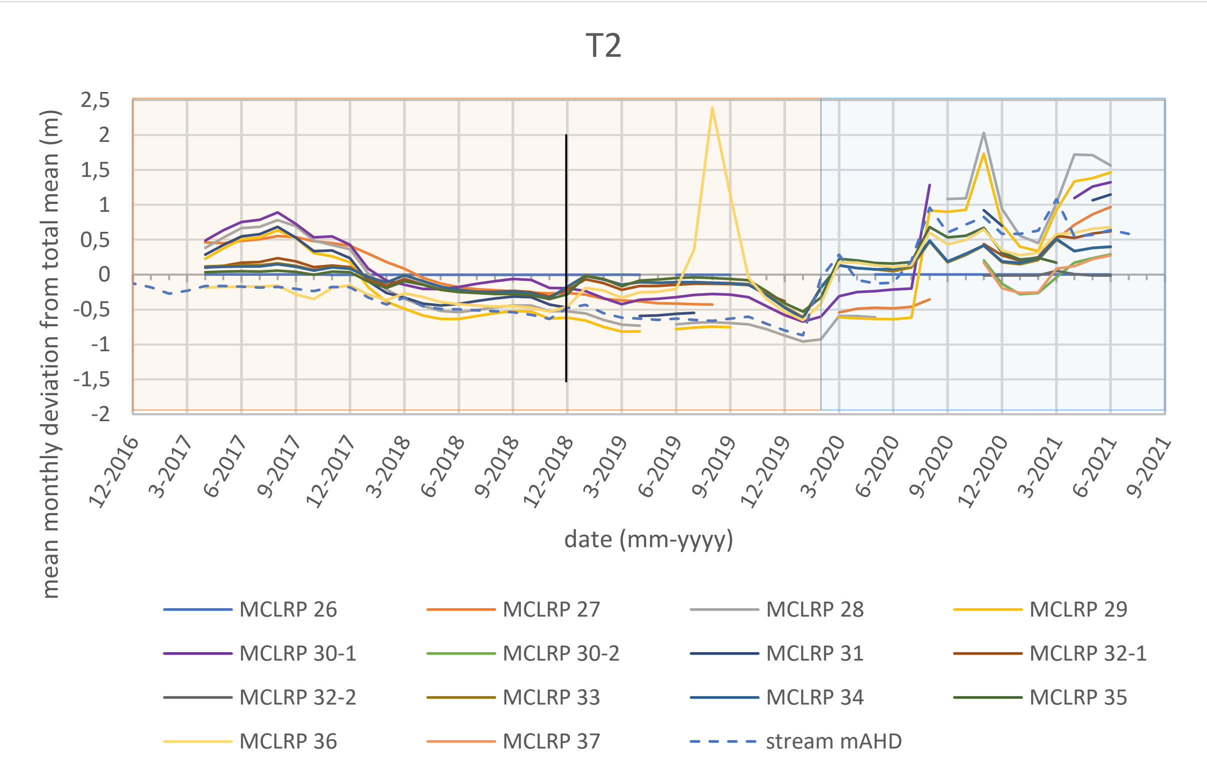

Figure 14 - mean monthly deviation from total mean in T2

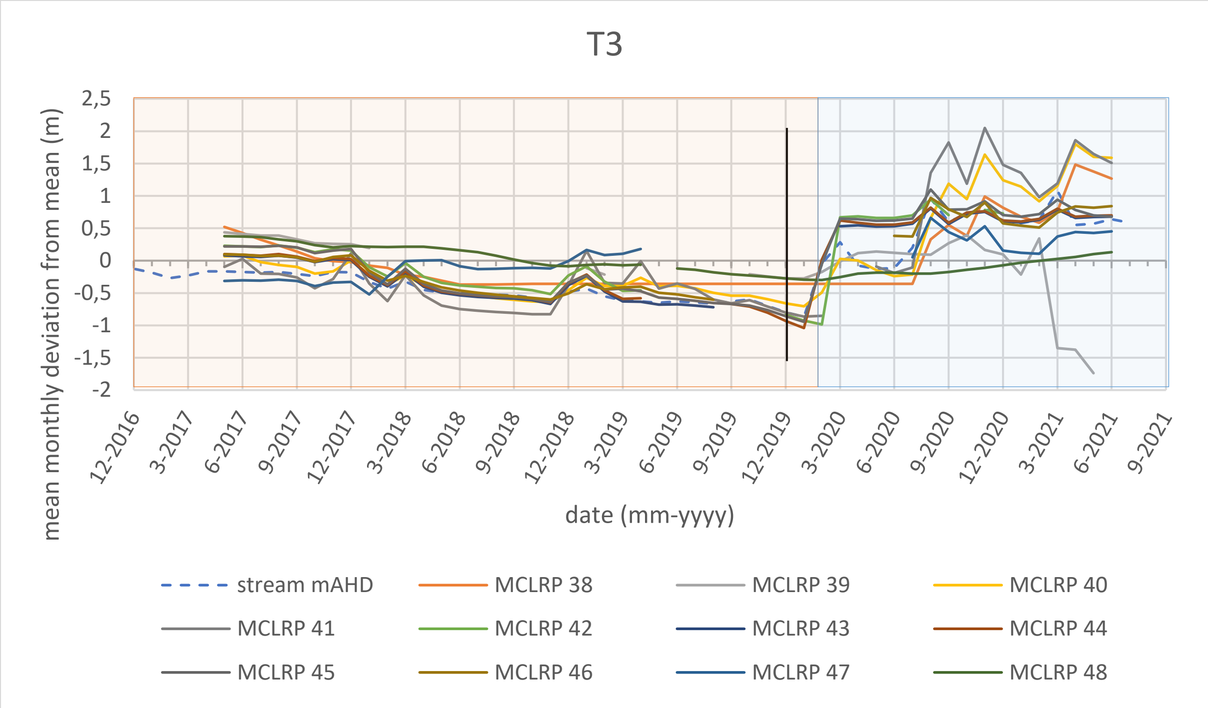

Figure 15 - mean monthly deviation from total mean in T3

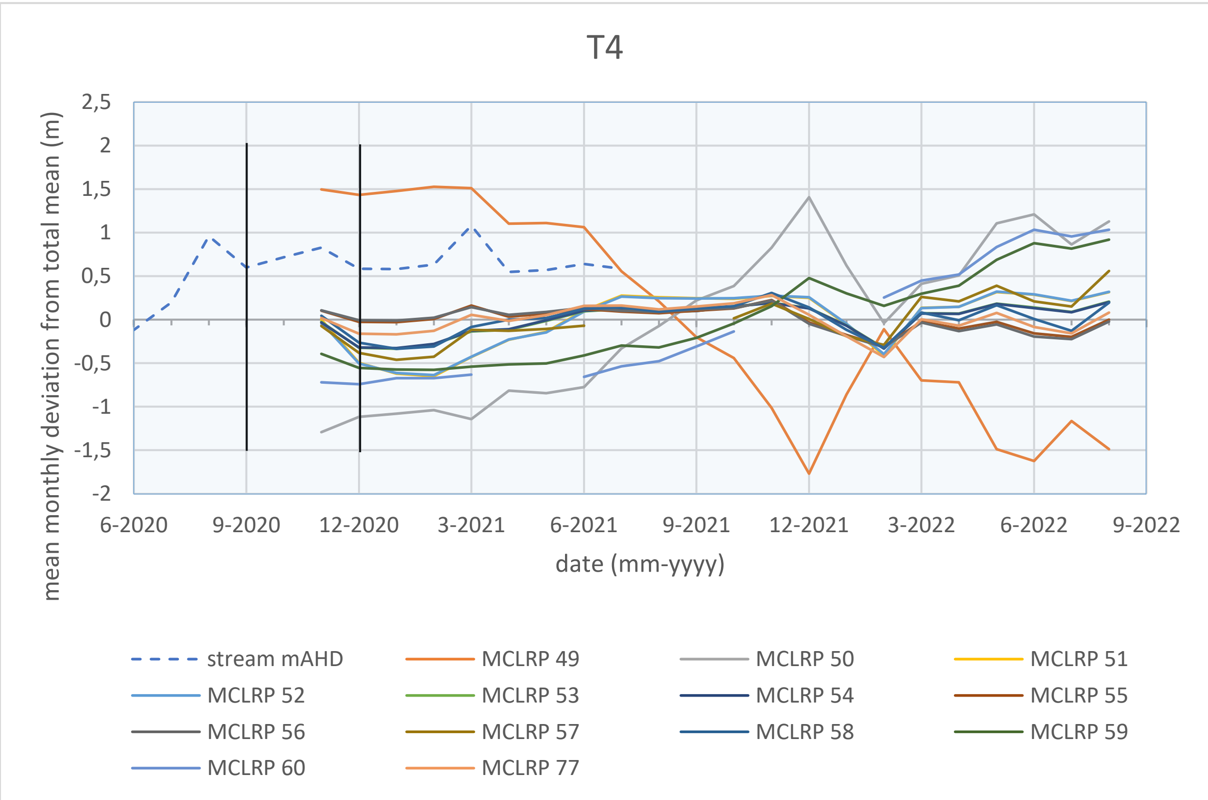

Figure 16 – mean monthly deviation from total mean in T4

7.2 Correlation matrix

The correlation matrix can be found in the appendix under 12.1, because it is too big fit in this chapter. The relevant results that are found in the matrix are discussed here. Regarding the table design, the matrix has a heatmap coloring, where green means the correlation coefficient is closer to 1 and red means the coefficient is closer to -1. The matrix is also split up into three parts and distributed over the three tables Table 10, Table 11 and Table 12. This is done for readability. Each of the three parts are treated as separate tables.

703 pairs of piezometers are evaluated, each of the 38 piezometers is also evaluated for their correlation with the stream water height and the two rain gauges are evaluated for their correlation. Table 3 summarizes all correlation coefficients higher than .85. This value is deemed as high. There are 207 pairs of piezometers that are correlated .85 or higher. That is 29% of all the pairs that are evaluated. This is not only a very large number, but it likely also contains a lot of pairs that are highly correlated by accident. The cross-correlation analysis and the recharge-discharge analysis both require a lot of time to do, so it is impossible to perform them on all 207 pairs. The correlations are depicted in Figure 13, where each pair of piezometers correlated .85 or higher is connected with a green line. This figure does not show much useful information, but it serves as an illustration of how many correlated pairs this is.

Table 3 - correlation coefficients higher than 0.85

r>0.85	T2	T3	T4
T2	37	-	-
T3	45	16	-
T4	66	24	19
Sum	**207**		

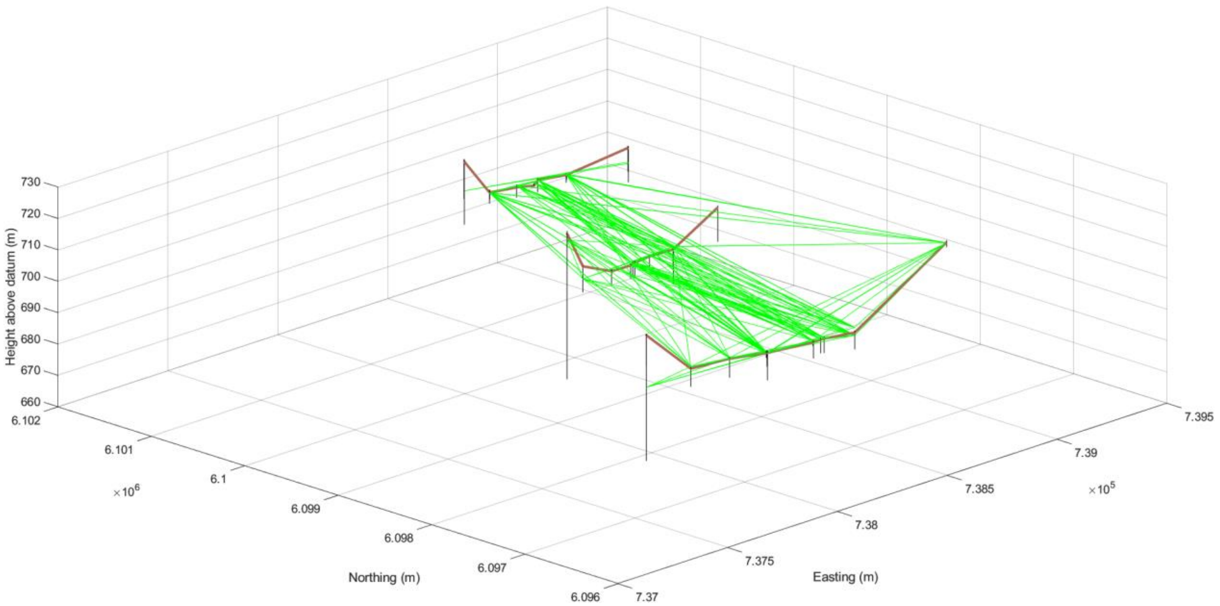

Figure 17 - all pairs of piezometers correlated 0.85 or higher in 3d space

To exclude some of the piezometer pairs from this list of 207, a selection is made. First, all piezometers that are correlated with the stream .85 or higher are included. This equates to 14 piezometers that will be called group A. The share from each transect is shown in Table 4. From there, all the piezometers with a

.85 correlation or higher with one of piezometers in group A were taken, however this resulted in 119 piezometer pairs and that was still too much. Therefore, the threshold was raised to a correlation of .95. This resulted in a group of 44 pairs of piezometers, which is called group B. To summarise, group B contains 44 pairs of piezometers that are either correlated .85 or higher with the stream or correlated .95 or higher to a piezometer that is correlated to the stream .85 or higher.

The 14 piezometers of group A and the 44 pairs of group B are shown in Table 5. The pairs of group B are plotted in 3d space in Figure 18 and as can be seen, the only pairs of piezometers that are left are pairs where both piezometers are in the floodplain, not in the ridges. This is good because the piezometers drilled in the ridges most likely are not affected by the leaky weirs anyway. The contribution of each transect to both group A and B is shown in Table 4.

Table 4 - pairs of piezometers correlated 0.95 or higher that are correlated with the stream 0.85 or higher

r with stream>0.85 + r >0.95	stream	T2	T3	T4
T2	5	9	-	-
T3	7	3	11	-
T4	2	14	6	1
Sum	**14**	**44**		

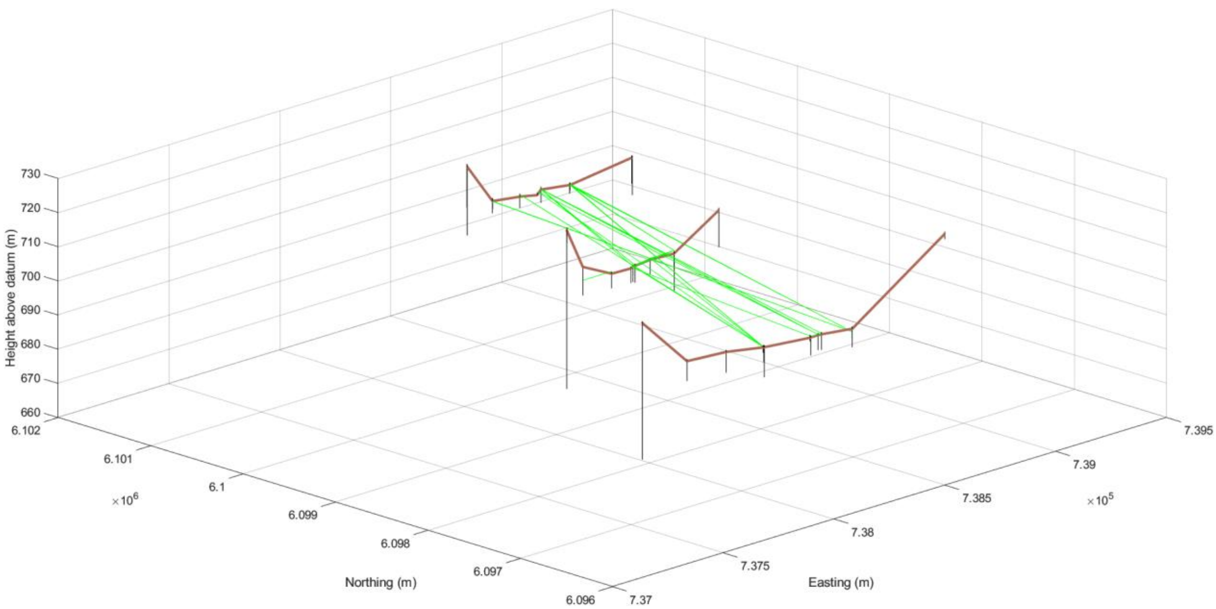

Figure 18 - pairs of piezometers correlated 0.95 or higher that are correlated with the stream 0.85 or higher

Table 5 - Piezometers in Group A and in Group B

Group A	Group B			
MCLRP 31	MCLRP 27	MCLRP 31	MCLRP 45	MCLRP 46
MCLRP 32-1	MCLRP 28	MCLRP 31	MCLRP 31	MCLRP 53
MCLRP 33	MCLRP 29	MCLRP 31	MCLRP 31	MCLRP 54
MCLRP 34	MCLRP 30-1	MCLRP 31	MCLRP 31	MCLRP 57
MCLRP 35	MCLRP 30-2	MCLRP 31	MCLRP 31	MCLRP 58
MCLRP 40	MCLRP 30-2	MCLRP 35	MCLRP 31	MCLRP 77
MCLRP 41	MCLRP 32-1	MCLRP 33	MCLRP 33	MCLRP 55
MCLRP 42	MCLRP 32-1	MCLRP 34	MCLRP 33	MCLRP 56
MCLRP 43	MCLRP 33	MCLRP 34	MCLRP 33	MCLRP 77
MCLRP 44	MCLRP 31	MCLRP 43	MCLRP 34	MCLRP 55
MCLRP 45	MCLRP 31	MCLRP 45	MCLRP 34	MCLRP 56
MCLRP 46	MCLRP 32-1	MCLRP 42	MCLRP 35	MCLRP 51
MCLRP 55	MCLRP 40	MCLRP 41	MCLRP 35	MCLRP 52
MCLRP 56	MCLRP 42	MCLRP 43	MCLRP 35	MCLRP 57
	MCLRP 42	MCLRP 44	MCLRP 35	MCLRP 58
	MCLRP 42	MCLRP 45	MCLRP 43	MCLRP 55
	MCLRP 42	MCLRP 46	MCLRP 43	MCLRP 56
	MCLRP 43	MCLRP 44	MCLRP 44	MCLRP 55
	MCLRP 43	MCLRP 45	MCLRP 44	MCLRP 56
	MCLRP 43	MCLRP 46	MCLRP 46	MCLRP 57
	MCLRP 44	MCLRP 45	MCLRP 46	MCLRP 58
	MCLRP 44	MCLRP 46	MCLRP 55	MCLRP 56

7.3 Cross-correlation

The results of the analysis are shown in Table 6. This table only holds those piezometer pairs that fulfil the two criteria set in section 6.3. The full table can be found in the appendix under 12.2. The full table is for all 44 pairs from group B, but after applying the two criteria the 8 pairs shown in Table 6 are left. From left to right, the table shows the two piezometers that make up the pair and to which transect they belong, then the statistics for the two criteria and lastly the median value of the calculated lag times.

From T2 to T4 there appears to be no lag time, but from T3 to T4 there appears to be about 1 hour of lag time. This indicates that there most likely is no flow between T2 and T4, but there may be flow between T3 and T4. However, the spatial configuration of the subsurface layers might be at the root of these differences. T2 and T4 are alike and therefore the water height in the piezometers in these transects respond to a rain event at a similar speed. T3 is different than T2 and T4, so the water height in the piezometers could be responding more quickly to a rain event than T2 and T4, explaining why T4 lags T3 by one hour. This is however just speculation and a tracer test like the one performed by DiLorenzo (2021) could give conclusive evidence on whether or not there is flow between transects.

MCLRP 42, 43 and 45 are all close to Mulloon creek, but MCLRP 45 lags 42 and 43 by 1 hour. A satellite image of all three piezometers is shown in Figure 19. 45 is on the other side of Mulloon creek, but still fairly close to the stream. What the cause is of this lag remains as of yet unknown.

Table 6 - lag times for inter-related group

P1	Transect P1	P2	Transect P2	Stdev (h)	Count (-)	Median (h)
MCLRP 33	2	MCLRP 34	2	0,32	18	0
MCLRP 31	2	MCLRP 54	4	0,35	8	0
MCLRP 31	2	MCLRP 57	4	1,22	9	-1
MCLRP 33	2	MCLRP 55	4	0,25	16	0
MCLRP 42	3	MCLRP 45	3	0,9	7	1
MCLRP 43	3	MCLRP 45	3	0,55	6	1,5
MCLRP 43	3	MCLRP 56	4	0,76	7	1
MCLRP 44	3	MCLRP 56	4	0,79	7	1

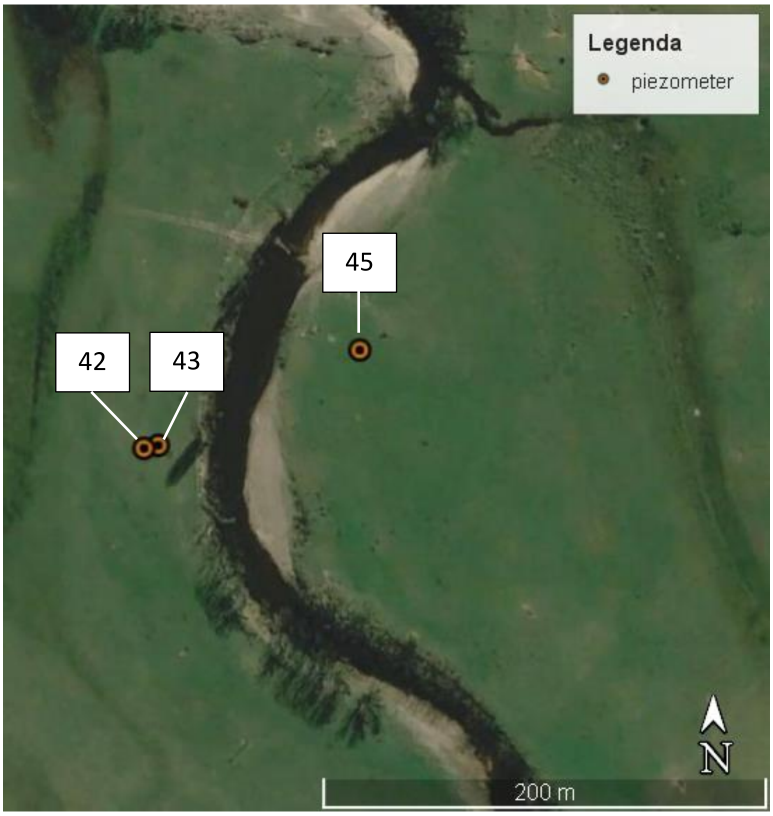

Figure 19 - MCLRP 42, 43 and 45 in T3

7.4 Recharge and discharge rates pre and post-leaky weirs construction

The method for calculating the recharge and discharge rates is explained in section 6.4 and the results are shown in Table 7 below. For each column of the period post leaky weir construction period, the coefficients are either colored red, green, or white compared to coefficients of the pre-leaky weir construction period. Red means the slope post-leaky weirs is lower than the slope pre-leaky weirs, minus 0.0005. Green means the slope post-leaky weirs is higher than the slope pre-leaky weirs, plus 0.0005. White means all other values. The value 0.0005 is included, because the piezometers only measure to an accuracy of 3 decimal points. 0.0005 is exactly half the accuracy of the piezometers. The coefficients for the discharge are in meters per day of drought and the coefficients for the recharge are in meters per millimeter of rain.

Table 7 - recharge and discharge slopes

	Discharge (m/d)		Recharge (m/mm)	
	pre	post	pre	post
MCLRP 31	-0,0011	0,0001	0,0032	0,0064
MCLRP 32-1	-0,0011	-0,0011	0,0110	0,0094
MCLRP 33	-0,0014	-0,0046	0,0029	0,0107
MCLRP 34	-0,0014	-0,0049	0,0030	0,0104
MCLRP 35	-0,0011	-0,0044	0,0005	0,0064
MCLRP 40	-0,0026	-0,0027	-0,0002	0,0047
MCLRP 41	-0,0045	-0,0046	0,0002	0,0078
MCLRP 42	-0,0024	-0,0025	0,0016	0,0064
MCLRP 43	-0,0022	-0,0019	0,0018	0,0072
MCLRP 44	-0,0038	-0,0034	0,0018	0,0111
MCLRP 45	-0,0050	-0,005	0,0012	0,0125
MCLRP 46	-0,0014	-0,0129	0,0013	0,0102

For the discharge, a green cell in the post-leaky weir column means that per day that there is no rain, the piezometer loses less height than it would have in the pre-leaky weir period. There is 1 piezometer for which this is the case, compared to 4 piezometers that show the opposite. Overall, the leaky weirs do not appear to slow down water leaving the aquifers. As discussed in section 7.3, one of the expected effects of leaky weirs was to slow down the water and keep it in the soil longer. If anything, there appears to be a slight increase in the rate at which the water is leaving.

This increase in discharge could be because the water in the piezometers is higher during the post-leaky weir period due to the wet period that began around the same time, as discussed in section 7.1. The higher discharge would then be due to a higher hydraulic gradient between the aquifer and the drainage point. This explanation assumes that the discharge rate used in this research is proportional to the slope of the hydraulic gradient, but testing this assumption is outside of the scope of this research and thus it is included in the recommendations under 10.3.

For the recharge, a green cell in the post-leaky weir column means that per millimeter that falls on a given day, the piezometer gains more height than it would have in the pre-leaky weir period. For all but one piezometer that is tested, there is a significant increase.

This column does support the hypothesis that leaky weirs slow down water. Slowing down water increases infiltration, which should result in a higher increase in water height in the piezometers relative to the amount of rain that falls, and that is exactly what can be seen in this analysis. Only piezometer MCLRP 32_1 shows a slight decrease. This piezometer is right next to MCLRP 33 and MCLRP 34 and the recharge rates for those piezometers did increase, so the spatial configuration does not explain why MCLRP 32_1 is not gaining water like its neighbors. Another explanation could be that there is no data for MCLRP 32-1 from the 9th of December 2019 to the 18th of November 2020. This means the change from dry to the wet period is not recorded and exactly this period might be the biggest factor in the change in recharge rate that is seen. The analysis in section 7.4.1 below elaborates further on the importance of this period of time for the recharge rates.

7.4.1 Transect 2 pre and post in the dry season

The change from a dry to a wet period could have a big influence on the discharge and recharge rates that have been calculated thus far. To get more accurate results, the variability in the weather data needs to be reduced. This can be done by only including the dry El Niño years from the dataset. As discussed in 7.1, on the 7th of February 2020 there was a big rain event, which will be used to mark the end of the La Niña phase and the beginning of the El Niño phase. Using this date and the dates from Table 2, only transect two can provide a big enough database for this analysis. For T2, the pre-leaky weir period spans from the 27th of April 2017 to the 1st of December 2018 and the post-leaky weir period spans from the 1st of December 2018 to the 7th of February 2020. The analysis was performed again for the piezometers of T2 and the results can be found in Table 8. A tolerance of 0.0005 was used, the same as it was before

Table 8 - T2 pre and post-leaky weir discharge and recharge

	discharge		recharge	
	pre	post	pre	post
MCLRP 31	-0,0011	-0,0004	0,0023	0,0007
MCLRP 32-1	-0,0011	-0,0002	0,0004	0,0004
MCLRP 33	-0,0014	-0,0022	0,0006	0,0006
MCLRP 34	0,0014	-0,0021	0,0007	0,0007
MCLRP 35	-0,0011	-0,0017	-0,0001	0,0003

What is apparent from Table 8 is that the leaky weirs do not seem to influence the recharge and discharge much, and not to the same degree that could be seen in Table 7. The discharge rates do seem to have improved compared to the previous analysis in the sense that the discharge rates for MCLRP 33, 34, and 35 have decreased less post-leaky weirs than pre-leaky weirs. The discharge rates for MCLRP 31 and 32-1 have increased more pre versus post-leaky weirs. So although in absolute terms the leaky weirs don't seem to have improved the discharge rates, compared to the previous analysis they have.

It should be mentioned that 2019 was the second dry year in a row and it came with big wildfires. The leaky weirs are likely not going to produce any positive results during a dry year, especially when it succeeds another, equally dry year. In the future, it would be wise to compare 2018 with another dry year that succeeds a wet year. This way, the circumstances between the two years are more equal and thus the results can be compared better. Similarly, it would be wise to compare 2020 with another year that succeeds a dry period to get the most accurate results.

8. Discussion

In general, the Mulloon catchment is a complex place where a lot of research has been done and data has been gathered. To do the data justice, the analyses done need to be automated, expanded and refined. Statistics need to be considered to determine whether results are significant and the configuration of the subsurface layers needs to be taken into account when interpreting the results. Tests with tracers most likely will be of more use than the cross-correlation analysis for determining flow between groundwater aquifers.

In this research, the gaps in the time series of some piezometers caused a massive loss of expected information. Had the process been automated, more piezometers could have been included in the cross-correlation analysis and this probably would have yielded more usable information.

For the recharge and discharge analysis, for now there is not enough data yet to determine the impact of the weather on the results. Therefore, the results are not valid. Also, in hindsight it would have been best to calculate the recharge and discharge rates for all piezometers. That way, the group with a connection to the stream (inter-correlated) can be compared to the group without a connection. Thus, changes between pre and post period in the inter-related group could be compared to changes in the group without a connection, thus determining if the leaky weirs had something to do with the changes or if the changes were due to the weather.

9. Conclusions

The first research question was 'is there flow between groundwater aquifers?'. The Pearson correlation analysis suggests there is more than likely some form of flow between some groundwater aquifers in the catchment, but this particular research failed to identify specific instances of this happen. The cross-correlation analysis showed that there might be flow between MCLRP 43 and 44 in T3 and MCLRP 56 in T4 because 56 lags 1 hour to the other two piezometers. The cross-correlation analysis also showed there is probably no flow between groundwater aquifers in T2 and T4.

The second research question was 'How much does the water height in the piezometers change after rain and after a dry period?'. The answer can be found in Table 7 and Table 8.
The third research question was 'How much has the change in water height in the piezometers after rain and after a dry period been affected by the placement of leaky weirs?'. When the whole time period is taken, the leaky weirs seem to significantly increase the recharge rate, but also slightly increase the discharge rate. This is probably due to the change in weather during the post-leaky weir period. When the analysis is limited to just the dry period, the increase in recharge rate disappears. This suggest that weather has a large influence on these recharge and discharge rates. That is why the analysis should be repeated in the future for two non-consecutive years with similar weather.

10. Recommendations

10.1 Negative correlations

Some pairs of piezometers display very high, negative correlations, see Table 9. This is strange and counterintuitive. Looking at Figure 20, MCLRP 49 seems to be the odd one out, behaving opposite to the other piezometers. It looks like the perfect opposite of 50, and it is pretty close to being the opposite of 59 and 60. This begs the question: why is MCLRP 49 behaving so differently?

Pair 35-50 can be partly explained because the datasets for both only overlap about 4 months. Seeing as correlation is taken for the data that overlaps, this negative correlation can be written off as a coincidence due to a small sample size.

Table 9 - negative correlations

Pair	correlation
35-50	-0,928
49-50	-0,996
49-59	-0,930
49-60	-0,948

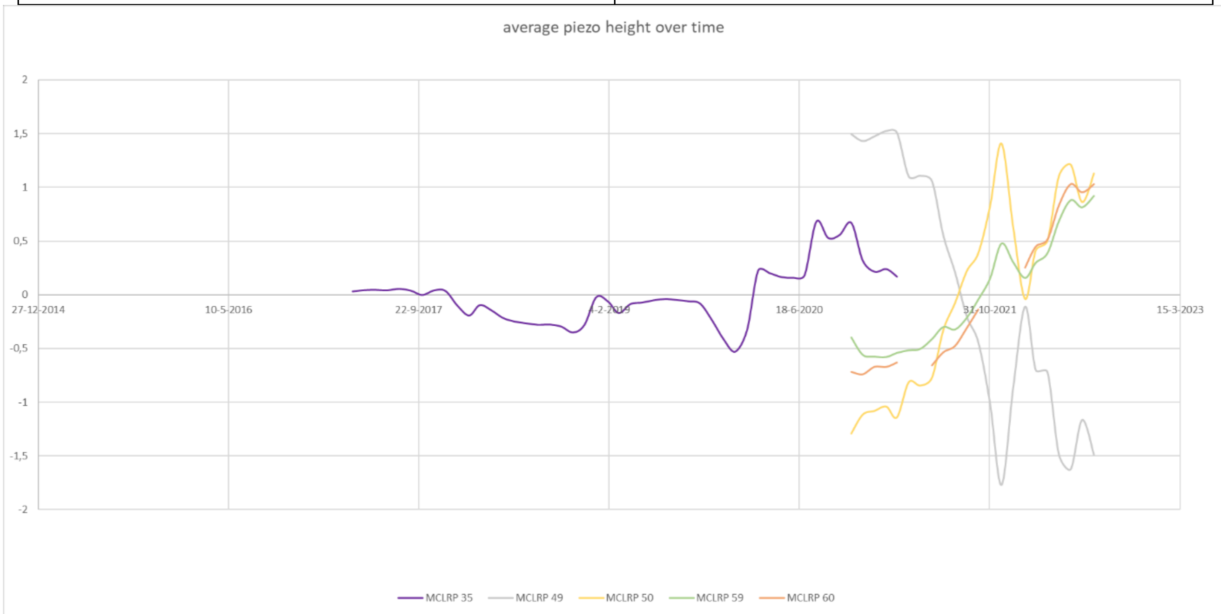

Figure 20 - negative correlations

10.2 Extremely high correlations

In the dataset, 16 pairs of piezometers correlate 0.99 or higher and 6 correlate 0.999 or higher. It could be useful to assess these pairs and see if one of the two piezometers in each pair might be redundant. This could free up instruments and reduce the maintenance load. A first start would be to check how much the datasets overlap, to avoid tainted results such as the 35-50 pair that only had a 4-month overlap.

10.3 Correlation with cumulative rainfall

In the future it is wise to also calculate a correlation coefficient between the piezometers and the cumulative rainfall. Calculating the coefficient with the normal rainfall yielded no high correlations, but throughout the whole research, the piezometers do seem to be affected by the rain.

10.4 MCLRP 36

MCLRP 36 has a strange spike between 1-6-2019 and 1-10-2019. The peak is around 6-9-2019. Between 22-6-2019 and 6-9-2019, the height rises steadily. After the 6th, the height stays somewhat constant up to 8-9-2019 at 14:00, when there is a sudden decline of 0.4m over 1.5 days until 10-9-2019 at 02:00 when the height drops by 3.4m in 6 hours. See Figure 21 for a picture of this sudden drop in height.

This looks like an unnatural event, so it is worth investigating whether the data is indeed realistic. Another explanation could be that MCLRP 36 is drilled into an aquifer that had its drainage blocked, causing an increase in pressure. The pressure eventually partly clears the blockade around 8-9-2019 at 12:00 and then fully around 10-9-2019 at 00:00. However, this is just speculation, and more research is required for a definitive answer.

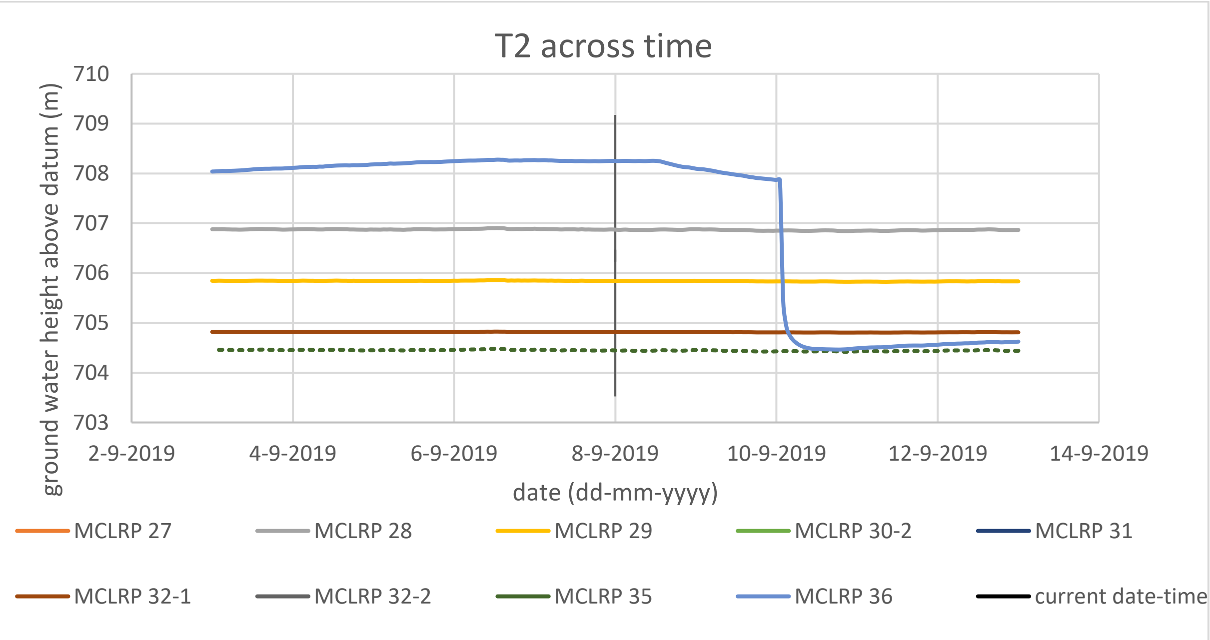

Figure 21 - sudden drop in MCLRP 36, a snapshot from 8-9-2019 00:00

10.5 Lag times

The table with lag times in 0 contains the lag times for all the piezometers pairs from the inter-related group. In the results section of this research, only those pairs with standard deviations of 2 or less were taken into account, but the pairs with higher standard deviations might still provide useful information. For example, MCLRP 42 and 46 have a median lag time of -6 hours with a standard deviation of -4.6 based on 7 data points. This does not say much about the magnitude of the lag time, but it could be taken as an indication of the sign. It could be reasonable to assume that there exists a negative lag time from 42 to 46, but how much this lag time is, is undetermined. Gathering these cases could provide an extra bit of insight into the subsurface flows. Knowing whether or not there is a positive, negative, or close-to-zero lag time can help.

Besides this, the method used could be elaborated much further. As proposed in 10.6 below, using Matlab would have produced a lot more data points. Right now, only days with a lot of rain are taken into account and each day has to be entered by hand. This takes a lot of time, but if MatLab was used, the calculations could have been done for all days, which probably would have resulted in more data points.

10.6 MatLab

The use of MatLab for a large part of these analyses would have made the whole research a lot more reproducible. It would have allowed for more flexibility in the formatting of the data and it would have made experiments more easily reproducible. Especially considering the complexity of the experiments such as calculating lag times and recharge and discharge coefficients, MatLab would have saved a lot of time.

11. References

Brierley, Gary J, Tim Cohen, Kirstie Fryirs, and Andrew Brooks. 1999. ‘European Changes to the Fluvial Geomorphology OfBega Catchment, Australia: Implications for Riverecology’. *Freshwater Biology* 41: 839–48.

Burch, G J, I D Moore, and J Burns. 1989. ‘Soil Hydrophobic Effects on Infiltration and Catchment Runoff’. *Hydrological Processes* 3(3): 211–22.

Dobes, Leo, Nathan Weber, Jeff Bennett, and Sue Ogilvy. 2013. ‘Stream-Bed and Flood-Plain Rehabilitation at Mulloon Creek, Australia: A Financial and Economic Perspective’. *Rangeland Journal* 35(3): 339–48.

Dunkerley, David. 2018. ‘How Is Overland Flow Produced under Intermittent Rain? An Analysis Using Plot-Scale Rainfall Simulation on Dryland Soils’. *Journal of Hydrology* 556: 119–30.

Hazell, Donna, Will Osborne, and David Lindenmayer. 2003. ‘Impact of Post-European Stream Change on Froghabitat: Southeastern Australia’. *Biodiversity and Conservation* 12: 301–20.

ICSM. 2022. ‘Geocentric Datum of Australia 2020’. *21-10-2022*. https://www.icsm.gov.au/gda2020 (October 28, 2022).

Johnston, Peter, and Gary Brierley. 2006. ‘Late Quaternary River Evolution of Floodplain Pockets along Mulloon Creek, New South Wales, Australia’. *Holocene* 16(5): 661–74.

L’Heureux, Michelle. 2014. ‘What Is the El Niño–Southern Oscillation (ENSO) in a Nutshell?’ *Climate.gov*: 1. https://www.climate.gov/news-features/blogs/enso/what-el-niño–southern-oscillation-enso-nutshell (November 7, 2022).

Nolan, R H et al. 2016. ‘Large-Scale, Dynamic Transformations in Fuel Moisture Drivewildfire Activity across Southeastern Australia’. *Geophysical Research Letters* 43(9): 4229–38.

Peel, Luke, Peter Hazell, Tony Bernardi, and Stephen Dovers. 2022. ‘The Mulloon Rehydration Initiative:The Project’s Establishment Andmonitoring Framework’. *Ecological Management and Restoration* 23(1): 25–42.

Scott, T. ‘Soil Erosion to Pasture Land near Tarlee in South Australia’.

Streeton, N A et al. 2013. ‘Rehabilitation of an Incised Ephemeral Stream in Central New South Wales, Australia: Identification of Incision Causes, Rehabilitation Techniques and Channel Response’. *Rangeland Journal* 35(1): 71–83.

12. Appendix

12.1 Correlation matrix

			T2													
		Stage_mAHD	*MCLRP 26*	*MCLRP 27*	*MCLRP 28*	*MCLRP 29*	*MCLRP 30-1*	*MCLRP 30-2*	*MCLRP 31*	*MCLRP 32-1*	*MCLRP 32-2*	*MCLRP 33*	*MCLRP 34*	*MCLRP 35*	*MCLRP 36*	*MCLRP 37*
	Stage_mAHD	1														
T2	MCLRP 26	0,696	1													
T2	MCLRP 27	0,521	0,483	1												
T2	MCLRP 28	0,822	0,725	0,931	1											
T2	MCLRP 29	0,806	0,659	0,874	0,995	1										
T2	MCLRP 30-1	0,744	0,638	0,938	0,983	0,992	1									
T2	MCLRP 30-2	0,271	0,243	0,548	0,935	0,962	0,994	1								
T2	MCLRP 31	0,890	0,687	0,951	0,984	0,993	0,999	0,992	1							
T2	MCLRP 32-1	0,886	0,697	0,841	0,932	0,949	0,923	0,856	0,949	1						
T2	MCLRP 32-2	0,465	-0,019	-0,282	0,358	0,404	-0,184	0,285	-0,341	0,613	1					
T2	MCLRP 33	0,865	0,628	0,536	0,789	0,810	0,740	0,667	0,898	0,969	0,555	1				
T2	MCLRP 34	0,875	0,633	0,511	0,788	0,800	0,728	0,642	0,896	0,968	0,547	0,999	1			
T2	MCLRP 35	0,879	0,620	0,127	0,795	0,778	0,541	0,983	0,809	0,926	0,312	0,894	0,902	1		
T2	MCLRP 36	0,414	0,258	0,106	0,297	0,287	0,142	0,884	0,714	0,366	0,547	0,463	0,470	0,572	1	
T2	MCLRP 37	0,393	0,184	0,304	0,888	0,925	0,877	0,906	0,912	0,890	0,405	0,727	0,707	0,934	0,910	1
T3	MCLRP 38	0,783	0,713	0,837	0,931	0,915	0,897	0,821	0,906	0,903	0,158	0,679	0,675	0,699	0,356	0,740
T3	MCLRP 39	-0,132	-0,170	-0,182	-0,027	-0,182	0,240	-0,243	0,451	-0,298	-0,107	-0,003	-0,007	0,186	-0,197	-0,248
T3	MCLRP 40	0,888	0,679	0,659	0,872	0,861	0,770	0,866	0,791	0,882	0,264	0,749	0,753	0,851	0,447	0,780
T3	MCLRP 41	0,883	0,638	0,551	0,841	0,823	0,698	0,729	0,724	0,846	0,273	0,752	0,757	0,880	0,456	0,671
T3	MCLRP 42	0,900	0,670	0,076	0,692	0,546	0,540	0,464	0,926	0,958	0,272	0,887	0,897	0,928	0,917	0,517
T3	MCLRP 43	0,928	0,741	0,406	0,773	0,707	0,603	0,541	0,951	0,917	0,543	0,854	0,866	0,879	0,431	0,623
T3	MCLRP 44	0,919	0,739	0,321	0,727	0,690	0,556	0,552	0,943	0,928	0,523	0,881	0,891	0,890	0,867	0,628
T3	MCLRP 45	0,924	0,742	0,425	0,775	0,743	0,619	0,452	0,953	0,925	0,747	0,873	0,879	0,889	0,372	0,598
T3	MCLRP 46	0,958	0,736	0,708	0,938	0,900	0,883	0,892	0,934	0,946	0,475	0,886	0,894	0,939	0,575	0,929
T3	MCLRP 47	0,663	0,348	-0,095	0,426	0,489	0,057	0,894	0,075	0,437	0,492	0,574	0,590	0,643	0,761	0,941
T3	MCLRP 48	0,019	0,040	0,771	0,401	0,205	0,689	0,462	0,449	0,323	0,076	0,203	0,185	-0,138	-0,238	0,449
T4	MCLRP 49	0,189	-0,355	-0,799	-0,540	-0,497	-0,534	-0,703	-0,805	-0,520	0,026	-0,163	-0,131	0,110	-0,448	-0,567
T4	MCLRP 50	-0,244	0,303	0,745	0,151	0,134	0,553	0,404	0,790	0,382	-0,028	-0,029	-0,050	-0,928	0,181	0,342
T4	MCLRP 51	0,227	0,152	0,532	0,964	0,959	0,801	0,914	0,847	0,841	0,345	0,616	0,592	0,964	0,866	0,944
T4	MCLRP 52	0,219	0,160	0,540	0,967	0,960	0,800	0,917	0,873	0,844	0,348	0,618	0,593	0,966	0,871	0,946
T4	MCLRP 53	0,475	0,159	0,268	0,796	0,872	0,966	0,904	0,988	0,903	0,367	0,840	0,826	0,903	0,928	0,900
T4	MCLRP 54	0,474	0,164	0,267	0,791	0,867	0,967	0,902	0,988	0,904	0,370	0,842	0,828	0,896	0,930	0,899
T4	MCLRP 55	0,880	0,056	-0,244	0,495	0,664	0,883	0,641	0,851	0,861	0,512	0,982	0,985	0,876	0,854	0,712
T4	MCLRP 56	0,871	0,078	-0,202	0,506	0,659	0,880	0,643	0,878	0,856	0,509	0,986	0,988	0,862	0,852	0,703
T4	MCLRP 57	0,542	0,141	0,053	0,894	0,952	0,813	0,923	0,955	0,947	0,458	0,823	0,805	0,984	0,965	0,943
T4	MCLRP 58	0,451	0,172	0,239	0,907	0,957	0,819	0,933	0,960	0,949	0,446	0,815	0,796	0,984	0,969	0,949
T4	MCLRP 59	0,220	0,071	0,470	0,665	0,714	0,753	0,754	0,725	0,745	0,481	0,438	0,422	0,816	0,600	0,754
T4	MCLRP 60	-0,076	0,002	0,343	-0,447	-0,431	-0,427	-0,399	0,157	-0,391	-0,033	-0,166	-0,152	-0,406	-0,348	-0,205
T4	MCLRP 77	0,659	0,127	0,005	0,654	0,776	0,960	0,785	0,964	0,931	0,496	0,953	0,946	0,904	0,932	0,843

Table 10 – part of the correlation matrix (1/3) with the stream gauge and the piezometers of T2 in the columns

		T3										
		MCLRP 38	*MCLRP 39*	*MCLRP 40*	*MCLRP 41*	*MCLRP 42*	*MCLRP 43*	*MCLRP 44*	*MCLRP 45*	*MCLRP 46*	*MCLRP 47*	*MCLRP 48*
T3	MCLRP 38	1										
	MCLRP 39	-0,255	1									
	MCLRP 40	0,930	-0,257	1								
	MCLRP 41	0,873	-0,199	0,973	1							
	MCLRP 42	0,536	0,426	0,742	0,737	1						
	MCLRP 43	0,697	-0,315	0,806	0,832	1,000	1					
	MCLRP 44	0,642	-0,025	0,786	0,828	1,000	1,000	1				
	MCLRP 45	0,685	0,007	0,804	0,842	0,991	0,992	0,990	1			
	MCLRP 46	0,869	-0,318	0,917	0,907	0,959	0,973	0,969	0,979	1		
	MCLRP 47	0,486	-0,313	0,662	0,731	0,332	0,614	0,585	0,578	0,640	1	
	MCLRP 48	0,285	0,232	0,056	-0,054	-0,023	-0,229	-0,026	0,053	-0,130	-0,590	1
T4	MCLRP 49	-0,877	0,501	-0,688	-0,430	0,458	0,020	-0,004	0,148	-0,434	-0,396	-0,748
	MCLRP 50	0,642	-0,436	0,356	0,098	-0,692	-0,185	-0,164	-0,300	0,140	0,103	0,818
	MCLRP 51	0,759	-0,064	0,857	0,803	0,311	0,527	0,527	0,565	0,909	0,901	0,211
	MCLRP 52	0,772	-0,077	0,864	0,802	0,319	0,524	0,524	0,560	0,913	0,904	0,234
	MCLRP 53	0,608	-0,103	0,694	0,593	0,714	0,762	0,767	0,658	0,927	0,937	0,379
	MCLRP 54	0,615	-0,115	0,693	0,587	0,718	0,761	0,767	0,654	0,925	0,935	0,400
	MCLRP 55	0,181	-0,087	0,345	0,338	0,927	0,978	0,978	0,843	0,810	0,840	0,229
	MCLRP 56	0,239	-0,093	0,379	0,345	0,944	0,980	0,982	0,838	0,805	0,834	0,237
	MCLRP 57	0,664	-0,184	0,786	0,704	0,816	0,741	0,744	0,707	0,974	0,975	0,314
	MCLRP 58	0,719	-0,183	0,811	0,723	0,415	0,727	0,731	0,692	0,975	0,975	0,335
	MCLRP 59	0,361	0,003	0,524	0,515	0,158	0,387	0,374	0,474	0,614	0,630	-0,048
	MCLRP 60	-0,545	-0,357	-0,412	-0,413	0,494	-0,198	-0,195	-0,254	-0,347	-0,326	0,637
	MCLRP 77	0,461	-0,146	0,554	0,473	0,791	0,905	0,909	0,788	0,902	0,916	0,385

Table 11 - part of the correlation matrix (2/3) with the piezometers of T3 in the columns

		T4												
		MCLRP 49	*MCLRP 50*	*MCLRP 51*	*MCLRP 52*	*MCLRP 53*	*MCLRP 54*	*MCLRP 55*	*MCLRP 56*	*MCLRP 57*	*MCLRP 58*	*MCLRP 59*	*MCLRP 60*	*MCLRP 77*
T4	MCLRP 49	1												
	MCLRP 50	-0,996	1											
	MCLRP 51	-0,683	0,688	1										
	MCLRP 52	-0,703	0,708	0,999	1									
	MCLRP 53	-0,586	0,591	0,925	0,925	1								
	MCLRP 54	-0,575	0,581	0,921	0,920	1,000	1							
	MCLRP 55	0,287	-0,264	0,262	0,250	0,492	0,505	1						
	MCLRP 56	0,350	-0,329	0,176	0,163	0,391	0,404	0,995	1					
	MCLRP 57	-0,670	0,655	0,874	0,876	0,874	0,870	0,304	0,192	1				
	MCLRP 58	-0,409	0,419	0,824	0,822	0,887	0,890	0,683	0,591	0,821	1			
	MCLRP 59	-0,930	0,910	0,598	0,615	0,517	0,53	-0,381	-0,445	0,707	0,292	1		
	MCLRP 60	-0,948	0,931	0,565	0,582	0,565	0,559	-0,494	-0,570	0,820	0,313	0,985	1	
	MCLRP 77	-0,081	0,103	0,600	0,593	0,775	0,784	0,919	0,873	0,585	0,869	-0,037	-0,047	1

Table 12 - part of the correlation matrix (3/3) with the piezometers of T4 in the columns

12.2 Cross-correlation table

P1	Transect	P2	Transect	Average (h)	Stdev (h)	Count (-)	Median (h)
MCLRP 27	2	MCLRP 31	2	7,67	3,79	3	6
MCLRP 28	2	MCLRP 31	2	-12	#DIV/0!	1	-12
MCLRP 29	2	MCLRP 31	2	-4	0	2	-4
MCLRP 30-1	2	MCLRP 31	2	-0,67	2,89	3	1
MCLRP 30-2	2	MCLRP 31	2	#DIV/0!	#DIV/0!	0	#NUM!
MCLRP 30-2	2	MCLRP 35	2	-5,5	9,19	2	-5,5
MCLRP 32-1	2	MCLRP 33	2	-9	2,86	11	-9
MCLRP 32-1	2	MCLRP 34	2	-9,1	2,96	10	-10
MCLRP 33	2	MCLRP 34	2	-0,11	0,32	18	0
MCLRP 31	2	MCLRP 43	3	#DIV/0!	#DIV/0!	0	#NUM!
MCLRP 31	2	MCLRP 45	3	#DIV/0!	#DIV/0!	0	#NUM!
MCLRP 32-1	2	MCLRP 42	3	-1,2	9,42	5	0
MCLRP 31	2	MCLRP 53	4	-1,08	6,33	13	-1
MCLRP 31	2	MCLRP 54	4	-0,13	0,35	8	0
MCLRP 31	2	MCLRP 57	4	-1	1,22	9	-1
MCLRP 31	2	MCLRP 58	4	6	4,97	9	4
MCLRP 31	2	MCLRP 77	4	-3,75	5,19	4	-2
MCLRP 33	2	MCLRP 55	4	-0,06	0,25	16	0
MCLRP 33	2	MCLRP 56	4	5,31	4,27	13	4
MCLRP 33	2	MCLRP 77	4	0,78	6,65	9	1
MCLRP 34	2	MCLRP 55	4	5,06	5,01	16	5
MCLRP 34	2	MCLRP 56	4	1	6,27	10	1,5
MCLRP 35	2	MCLRP 51	4	-2,42	4,96	12	-2
MCLRP 35	2	MCLRP 52	4	#DIV/0!	#DIV/0!	0	#NUM!
MCLRP 35	2	MCLRP 57	4	#DIV/0!	#DIV/0!	0	#NUM!
MCLRP 35	2	MCLRP 58	4	#DIV/0!	#DIV/0!	0	#NUM!
MCLRP 40	3	MCLRP 41	3	#DIV/0!	#DIV/0!	0	#NUM!
MCLRP 42	3	MCLRP 43	3	#DIV/0!	#DIV/0!	0	#NUM!
MCLRP 42	3	MCLRP 44	3	0	0	2	0
MCLRP 42	3	MCLRP 45	3	0,86	0,9	7	1
MCLRP 42	3	MCLRP 46	3	-4,57	6,27	7	-6
MCLRP 43	3	MCLRP 44	3	1	0	2	1
MCLRP 43	3	MCLRP 45	3	1,5	0,55	6	1,5
MCLRP 43	3	MCLRP 46	3	#DIV/0!	#DIV/0!	0	#NUM!
MCLRP 44	3	MCLRP 45	3	11	#DIV/0!	1	11
MCLRP 44	3	MCLRP 46	3	-2	#DIV/0!	1	-2
MCLRP 45	3	MCLRP 46	3	-1	1,41	2	-1
MCLRP 43	3	MCLRP 55	4	1	0	2	1
MCLRP 43	3	MCLRP 56	4	1,29	0,76	7	1
MCLRP 44	3	MCLRP 55	4	2	0	2	2
MCLRP 44	3	MCLRP 56	4	1,43	0,79	7	1
MCLRP 46	3	MCLRP 57	4	-1	2,31	4	-1
MCLRP 46	3	MCLRP 58	4	2	4,8	7	1
MCLRP 55	4	MCLRP 56	4	0	0	2	0

12.3 Raw data, calculations, graphs, and tables

The raw data, calculations, graphs and tables that are explained and shown in this report can be found in the three excel files in the zip-folder that also contained this pdf document.

The file 'The Big Analysis Worksheet for Final delivery' contains the raw data for all data sources, the correlation matrix, the Group B selection process and the cross correlation calculations.
The raw data can be found in the tabs with a name that starts with 'data…'.
The correlation matrix can be found under the tab 'correlation matrix'. This sheet also contains the calculations for determining the size group B.
The piezometers belonging to group B can be found under the tab 'Group B'.
The calculations for the cross-calculation analysis can be found under the tab 'cross-correlation'. The process of calculating lag times involved entering a time and date of a rain event into the B2 cell of the tab 'hourly data graphs' and then the lag times for the 10-day interval around that date and time appeared in AO58:AO101 in the sheet under tab 'cross-correlation'.
The file also contains two tabs called 'filtered data for graphs' and 'hourly data graphs'. These are not discussed in this report, but they are essential for the Group B selection process and the cross-correlation calculations. Therefore, they are left in the file, but they can be ignored.

The file 'mean monthly deviations from mean' contains the graph shown in section 7.1 and also the raw data for the piezometers, stream gauge and rain gauges. The sheets that are used by the graphs are under the tabs named 'mean monthly dev' or 'mmd…', where mmd stands for mean monthly deviation (from total mean). There is also a tab that is called 'avg&sum rain gauge', which contains the average and sum per month that the rain gauges recorded data. This sheet is not used much in this report, but there is a reference to it in the mean monthly deviation calculations, so it is essential to include it in the file.

The last file is the 'recharge and discharge rate calculations'. This file contains the raw data from the appropriate piezometers and the sandhills rain gauge. This raw data is read by the 'difference per day' tab, which performs the appropriate calculations to get the required format. This is then copy pasted into the table in the sheet under tab 'results from calculation'. This table can then be sorted for the appropriate time period. This table is then used by the graphs under the tabs 'graphs whole data series' and 'graphs T2 dry period'. These graphs calculate a trendline for the data that they display and the slope of the trendline is manually recorded in the tables in the sheet under the tab 'trendline coefficients' in the columns under the letter 'a'. The intercepts of the trendlines are also recorded in the columns under the letter 'b', but these are not used in this report.